2022-01-0973 Published 15 Jun 2022

Analytical and Numerical Models of the Sound Radiated by Fully Clamped Rectangular Vibrating Plates

Anna Tira, Daniel Pinardi, Costante Belicchi, and Angelo Farina University of Parma

Alessio Figuretti and Stefano Izzo McLaren Automotive

Citation: Tira, A., Pinardi, D., Belicchi, C., Farina, A. et al., "Analytical and Numerical Models of the Sound Radiated by Fully Clamped Rectangular Vibrating Plates," SAE Technical Paper 2022-01-0973, 2022, doi:10.4271/2022-01-0973.

Received: 08 Dec 2021 Revised: 01 Apr 2022 Accepted: 06 Apr 2022

Abstract

In the present work, fully clamped rectangular isotropic plates are investigated: the response under steady-state excitation determined by harmonic point force application is calculated, and the consequent sound radiation is evaluated.

The study is carried out both analytically and numerically. At first, the analytical solution of the clamped-clamped plate motion equation is calculated by means of a MATLAB implementation. The solution is based on the Principle of Virtual Work, calculating the displacement as a function of frequency at the nodes of a rectangular mesh. The monopole approximation of Rayleigh's integral is then used to estimate the sound radiation in free field propagation. The numerical solution is evaluated using COMSOL Multiphysics, employing the Finite Elements Method (FEM). The clamped plate is modeled as a shell and "Acoustic-Structure Boundary" coupling is employed.

Furthermore, the optimization of force application point is performed, with the aim of maximizing the radiated sound pressure level or flattening the frequency response. Very good matching between analytical and numerical methods has been found. In conclusion, a reliable prediction model of the sound pressure radiated by clamped plates in the low frequency range is achieved.

Keywords

analytical, clamped, fem, isotropic, numerical, plates, Rayleigh's integral, sound radiation, vibration

I. Introduction

Sound radiators based on forced vibrations of a plate are becoming widely employed in the automotive field, where a trend of avoiding loudspeakers use for active sound reinforcement and noise cancelling systems is observed [1, 2]. The authors are employing the outcome of the presented work for the development of a pedestrian alert system (AVAS): vibrating panels provided with shakers are used for controlling the sound field outside the vehicle.

The sound radiation of panels can be computed once the velocity of each point of the panel is known, as a response to the force applied in one point. Therefore, the analytical solution of the motion equation is required and depends on the boundary conditions. Numerous studies about dynamic response of plates with various boundary conditions can be found in literature (a wide amount of work has been produced by Leissa [3, 4]) and the classical solution approaches are the Rayleigh-Ritz and superposition methods [5, 6, 7].

In this work, the plate in clamped condition is analyzed, and the Principle of Virtual Work is used, based on the approach explained in [8, 9], though the explicit formulae are reported in [10]. The fundamentals of this method were introduced in [11]. As regards the sound radiation generated by the vibrating plate, it can be analyzed by the monopole approximation of Rayleigh's integral. In fact, it provides an accurate approximation of the sound pressure in far field condition for relatively flat geometries operated in an infinite baffle [12, 13]. In details, the panel operates in free field and is clamped at the center of a rigid baffle that "splits" in two half-spaces the air surrounding the plate. The Rayleigh's formula considers sound propagation in one of these half spaces.

The analytical solution of the problem is calculated implementing the equations in MATLAB. Then, the results are compared with a numerical model obtained in COMSOL Multiphysics, employing FEM. To have truly comparable solutions, the input parameters (e.g., mesh and frequency resolutions, evaluation distance, material properties) are set equal.

In both cases, the output consists in a chart of Sound Pressure Level (SPL) vs frequency. To provide more reliable results, the SPL values are averaged over a grid of points, located at 1 meter distance from the plate.

A very good matching between analytical and numerical solutions is shown, thus cross validation of the two methods is achieved. Furthermore, the problem of identifying the optimal application point of the exciting force is investigated, showing that the maximum A-weighted SPL is obtained applying the force at the center of the plate. In addition, a different optimization of the excitation point is performed, with the aim of providing the flattest frequency response.

The paper is organized as follows. In section II, the theoretical basis of the analyzed problem is provided. In section III, the analytical and numerical methods are described. In section IV and V, results are shown and compared, and section VI summarizes the conclusions.

II. Theoretical Background

A. Solution of Motion Equation for Fully Clamped Rectangular Plates

The motion equation of forced vibrations of a thin un-damped rectangular clamped plate, made of isotropic material with length a, width b and thickness h is:

$$B\left(\frac{\partial^4}{\partial x^4}+2\frac{\partial^4}{\partial x^2\partial y^2}+\frac{\partial^4}{\partial y^4}\right)w(x,y,t)+\rho h\frac{\partial^2 w(x,y,t)}{\partial t^2}=p_{ext}(x,y,t) \tag{1}$$

where $B=\frac{Eh^3}{12(1-\nu^2)}$ is the bending stiffness of the plate, w is the displacement along z axis at point (x, y), ν is the Poisson's ratio, E is the Young's modulus, ρ is the density of plate and p_{ext} is the applied harmonic force. Letting:

$$w(x,y,t)=W(x,y)e^{i\omega t} \tag{2}$$

and

$$p_{ext}(x,y,t)=P(x,y)e^{i\omega t} \tag{3}$$

the equation becomes:

$$B\left(\frac{\partial^4}{\partial x^4}+2\frac{\partial^4}{\partial x^2\partial y^2}+\frac{\partial^4}{\partial y^4}\right)W(x,y)-\rho h\omega^2 W(x,y)-P(x,y)=0 \tag{4}$$

Expanding W and P as the superposition of adequate shape functions [8, 9] one obtains:

$$W(x,y)=\sum_{m=1}^{\infty}\sum_{n=1}^{\infty}W_{mn}\psi_{mn}(x,y) \tag{5}$$

$$P(x,y)=\sum_{m=1}^{\infty}\sum_{n=1}^{\infty}P_{mn}\psi_{mn}(x,y) \tag{6}$$

The shape functions can be decomposed as:

$$\psi_{mn}(x,y)=X_m(x)Y_n(y) \tag{7}$$

where X_m and Y_n are eigenfunctions that satisfy the boundary conditions of the plate, which are $w=\frac{\partial w}{\partial z}=0$ for fully clamped plates. Applying the Virtual Work Principle, one gets:

$$\int_0^a\int_0^b\left[B\left(\frac{\partial^4}{\partial x^4}+2\frac{\partial^4}{\partial x^2\partial y^2}+\frac{\partial^4}{\partial y^4}\right)W(x,y)-\rho h\omega^2 W(x,y)-P(x,y)\right](\delta W)dxdy=0 \tag{8}$$

where the virtual displacement is:

$$\delta W=\sum_{k=1}^{\infty}\sum_{k=1}^{\infty}\delta W_{ik}\psi_{ik}(x,y) \tag{9}$$

After few mathematical steps that can be found in [8, 9, 10] one obtains the dynamic response $W(x, y)$ of a plate subjected to a harmonic point force:

$$W(x,y)=\sum_{m}^{\infty}\sum_{n}^{\infty}\frac{PX_m(\xi)Y_n(\eta)}{D(I_1I_2+2I_3I_4+I_5I_6)-\rho h\omega^2 I_2I_6}X_m(x)Y_n(y) \tag{10}$$

B. Sound Pressure Evaluation with Rayleigh's Integral

Due to the acoustic radiation occurring on the surface of the plate, an acoustic pressure $P(\boldsymbol{r}_2,f)$ as a function of the frequency f at a point $\boldsymbol{r}_2$ located in air, at a significant distance from the plate can be calculated by Rayleigh's integral [8, 9, 12]:

$$P(\boldsymbol{r}_2,f)=\frac{j\omega\rho_0}{2\pi}\int_{dS}v(\boldsymbol{r}_1)\frac{e^{-ik|\boldsymbol{r}_2-\boldsymbol{r}_1|}}{|\boldsymbol{r}_2-\boldsymbol{r}_1|}dS \tag{11}$$

where ρ_0 is the air density, ω is the angular frequency of the plate, k is the wave number, S is the plate surface and $|\boldsymbol{r}_2-\boldsymbol{r}_1|$ is the distance between the calculation point in air and the radiation point $\boldsymbol{r}_1$ on the surface. It is possible to discretize the rectangular plate into N elements of areas ΔS, and thus to approximate the surface integral by a finite number N of surface elements with known properties:

$$P(\boldsymbol{r}_2,f)=\frac{j\omega\rho_0}{2\pi}\sum_{n=1}^{N}v(\boldsymbol{r}_n)\frac{e^{-ik|\boldsymbol{r}_2-\boldsymbol{r}_n|}}{|\boldsymbol{r}_2-\boldsymbol{r}_n|}\Delta S_n \tag{12}$$

The resulting sound pressure level can be obtained:

$$SPL(\boldsymbol{r}_2,f)=20log\left(\frac{|P(\boldsymbol{r}_2,f)|}{p_0}\right)[dB] \tag{13}$$

where $p_0 = 20\ \mu Pa$ is the reference sound pressure.

It is also possible to define an accumulated acceleration [12], which neglects the phase information:

$$aa(\boldsymbol{r}_2,f)=\frac{j\omega\rho_0}{2\pi}\int_{dS}\frac{|v(\boldsymbol{r}_1)|}{|\boldsymbol{r}_2-\boldsymbol{r}_1|}dS \tag{14}$$

and the corresponding Accumulated Acceleration Level (AAL):

$$AAL(\boldsymbol{r}_2,f)=20log\left(\frac{aa((\boldsymbol{r}_2,f))}{p_0}\right)[dB] \tag{15}$$

The AAL summarizes the total vibration of the radiator from an energetic point of view. AAL and SPL curves are identical up to the break-up frequency, i.e., as long as the surface of the radiator moves in-phase (pistonic motion). Above the break-up, acoustic cancellation phenomena occur, and the SPL becomes always lower than the AAL.

A mean SPL value can be calculated for estimating the average pressure level produced by a vibrating plate at the point $\boldsymbol{r}_2$, allowing to compare different excitation points, and thus to optimize the force application position, as described in section V. The mean SPL value can be obtained as:

$$SPL_{avg}(\boldsymbol{r}_2)=20log\left(\frac{\sqrt{\frac{1}{n_f}\sum_f|P(\boldsymbol{r}_2,f)|^2}}{p_0}\right) \tag{16}$$

where n_f is the number of frequencies. One can note that the numerator of (16) is the *rms* pressure. If A-weighting filter is applied, $SPL_{avg(A)}(\boldsymbol{r}_2)$ is obtained.

III. Analytical and Numerical Models

Relying on [14, 15], the analytical solution of the motion equation of forced vibrations of a thin isotropic un-damped rectangular clamped plate was implemented in form of a MATLAB script.

An aluminum plate with dimensions $a = 0.3$ m, $b = 0.2$ m and thickness $h = 1$ mm was studied, having the following mechanical properties: density $\rho = 2710\ kg/m^3$, Poisson's ratio $\nu = 0.33$ and Young's modulus $E = 70\ GPa$. The frequency range of interest was between $f_{min} = 150\ Hz$ and $f_{max} = 1\ kHz$, with frequency resolution $\Delta f = 2\ Hz$. The magnitude of the exciting force was $F = 1\ N$. Air properties required for solving the Rayleigh's integral were the following: $\rho_{air} = 1.2\ kg/m^3$ and speed of sound $c = 343\ m/s$.

A rectangular grid was generated to discretize the plate: the spatial resolution of the mesh must have at least 6 points per wavelength to provide a correct solution [16]. Considering the frequency range of interest in this work, the maximum size of the elements would be about 0.057 m. It was opted to use a mesh resolution $\Delta s = 0.03\ m$, thus obtaining a total number of elements equal to $N = 60$. Hence, the normal displacement matrix was calculated: it contains each node's displacement in the normal direction caused by the application of the harmonic force, as can be seen in Fig. 1, for the 400 Hz frequency and force applied at the center.

Afterwards, exploiting plate's symmetry, the exciting force was applied to all the nodes in the first quadrant of the mesh grid, sweeping them one by one and storing the solutions separately. The nodes on the edge of the plate were not excited, since they respect the boundary condition of fully clamped

FIGURE 1 Aluminum plate deformation at 400 Hz caused by the application of a 1 N harmonic force at its center.

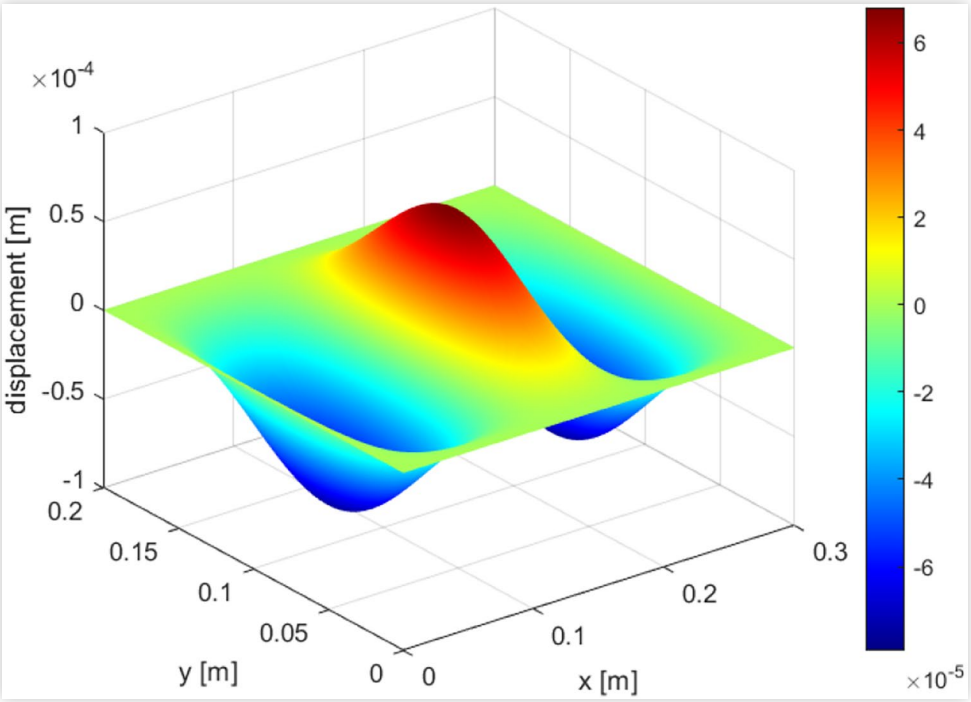

FIGURE 2 Mapped mesh with N = 60 elements for the numerical model of the plate, COMSOL Multiphysics.

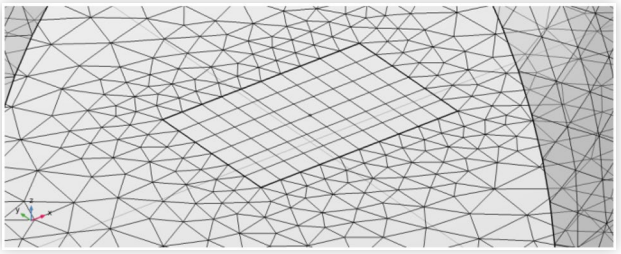

plate, i.e., they are fixed. To calculate the Rayleigh's integral, the displacement matrix was derived, obtaining the normal velocity of the nodes at every frequency. Then, sound pressure and accumulated acceleration were calculated with (12) and (14) and converted to SPL and AAL curves with (13) and (15), respectively.

The numerical solution of the problem addressed in the present paper was obtained with a simulation in COMSOL Multiphysics. The model employed two modules, Pressure Acoustic - Frequency Domain and Solid Mechanics, related by the Acoustic-Structure boundary coupling. The plate was modeled as an aluminum shell having the previously described dimensions, clamped on a rigid baffle, and surrounded by an air sphere of 1 m radius. Material properties of aluminum and air were identical to the analytical solution. The rigid baffle was defined as "interior sound hard boundary" [16] and the radiation boundary condition for the air domain was "spherical wave radiation" [16]. To have the best possible accordance between analytical and numerical models, the plate was subdivided in a rectangular mesh, namely a "mapped" mesh, having the same number and dimensions of the elements in the analytical solution. The rigid baffle was meshed with "free triangular" elements, while "free tetrahedral" elements were used for the air (Fig. 2).

The simulation was calculated in the same frequency range and resolution of the analytical study, hence $f_{min} = 150\ Hz$ and $f_{max} = 1\ kHz$, with a frequency resolution of $\Delta f = 2\ Hz$. Also in this case, a unit force $F = 1\ N$ normal to the plate was applied at all the nodes of the first quadrant of the mesh, one at a time. Results were obtained in terms of AAL and SPL curves as a function of the frequency.

Finally, the effect of damping, which is always present in real systems, was introduced in the numerical model. It was defined as isotropic loss factor, having value $\eta = 0.05$. Damped and undamped numerical solutions are compared in this paper. The analysis will be extended to experimental results in subsequent works.

IV. Comparative Analysis of the Analytical and Numerical Results

At first, AAL and SPL curves were calculated on-axis at one meter distance solving the analytical model. In Fig. 3 an example is shown for force applied at point ($x = 0.21\ m; y = 0.1\ m$). It is possible to observe the break-up at 200 Hz, where AAL and SPL curves diverge due to the acoustic cancellation. One can also note the resonance peaks which tend to infinite due to the absence of damping in the analytical solution.

Despite the evaluation at 1 m distance on-axis in front of the panel is a typical approach, it may result in misleading responses. In fact, it lacks important phase information of the radiated sound, resulting in a poorly realistic prediction of the generated sound field. For a practical use of the proposed method to evaluate the sound pressure produced by a vibrating plate, it must be considered that the listener could be standing in another position, for example out of the z-axis. For this reason, (12) and (14) were solved on a grid of 45 observation points arranged on a semi-sphere of radius $r = 1\ m$ concentric with the plate, as shown in Fig. 4, and then averaged.

In Fig. 5, it is clearly noticeable how space averaging can affect the results: some peaks of the AAL curve that were not present in the SPL curve of Fig. 3 (calculated only in one point on-axis) are now visible in the SPL curve. The average over the observation grid therefore allows a more realistic evaluation.

Then, the results obtained by the analytical and numerical models were compared. Fig. 6 shows the residual curves obtained by subtracting the SPL curves calculated by the two methods. The solutions were computed in both cases by exciting all the free points in the first quadrant of the mesh, which are 15 with the chosen discretization, and averaging each result over the grid of 45 observation points at 1 m distance. One can note that all the residual curves are in the range $\pm 3\ dB$. The peaks in the residual curves correspond to the theoretically undamped resonance frequencies. Considering the good agreement obtained, it is possible to state that the two methods are validated and can be successfully employed for further studies.

Eventually, a numerical simulation was performed by introducing damping as an isotropic loss factor $\eta = 0.05$. In Fig. 7 it is possible to see the comparison between damped and undamped cases, for a force of 1 N applied at point ($x = 0.21\ m; y = 0.1\ m$) and evaluated at the observation grid. One can note the effect of damping in correspondence of the resonance frequencies, where the peaks are smoothed instead of going to infinite, as it happens in real systems.

FIGURE 3 AAL (dash line) and SPL (solid line) curves, evaluated in a point on-axis at 1 m distance. Analytical solution, force applied in *(x, y) = (0.21 m, 0.1 m)*.

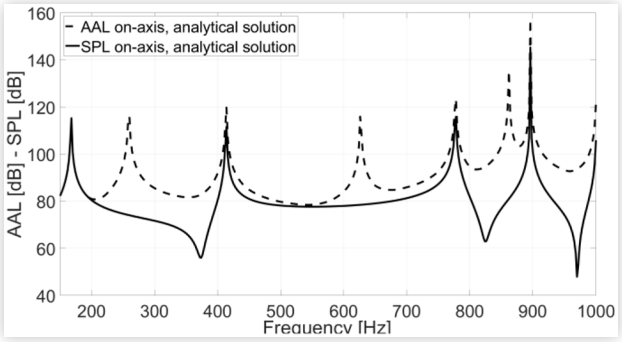

FIGURE 4 Grid of 45 observation points on a sphere of radius *r=1m*, centered with the plate.

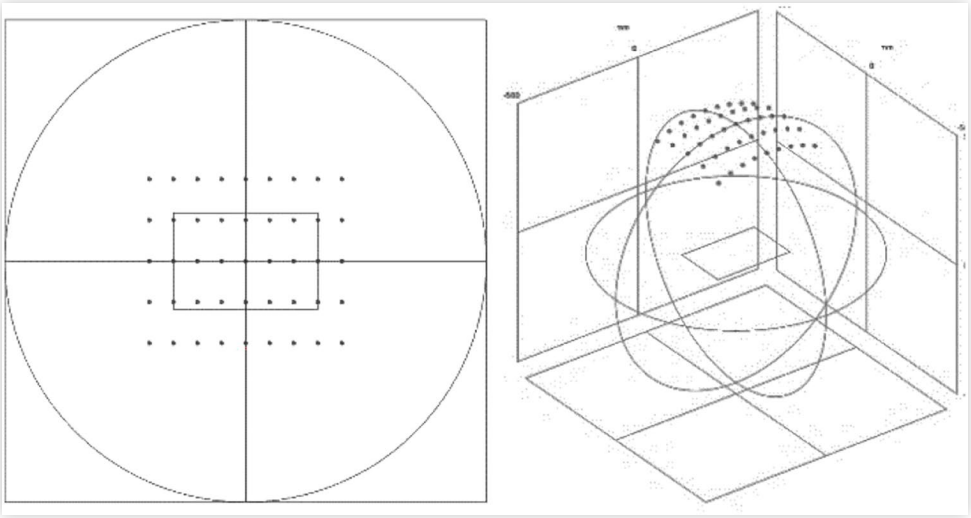

FIGURE 5 AAL (dash-dot line) and SPL (dot line) curves evaluated in one point on-axis at 1 m distance, and SPL (solid line) curve averaged over 45 observation points. Analytical solution, force applied in *(x, y) = (0.21 m; 0.1 m)*.

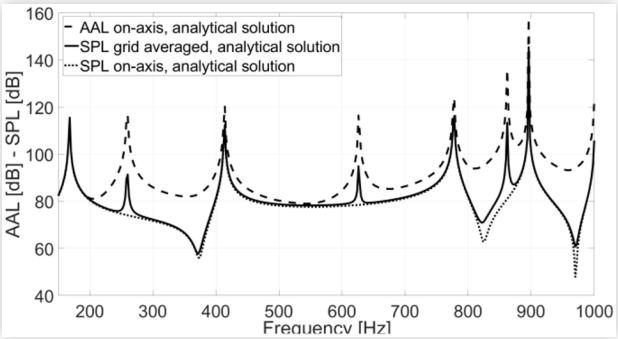

FIGURE 6 SPL curves averaged over 45 observation points, residual of the difference between analytical and numerical solutions. Force applied in all free points of first quadrant.

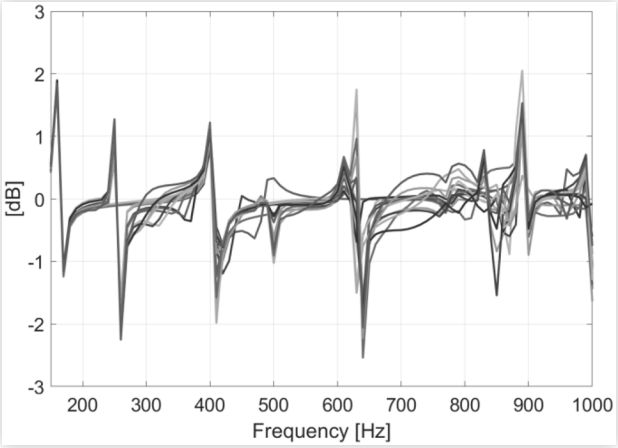

FIGURE 7 SPL undamped (solid line) and SPL damped (dot line) curves averaged over 45 observation points, numerical model, force applied in *(x, y) = (0.21 m; 0.1 m)*.

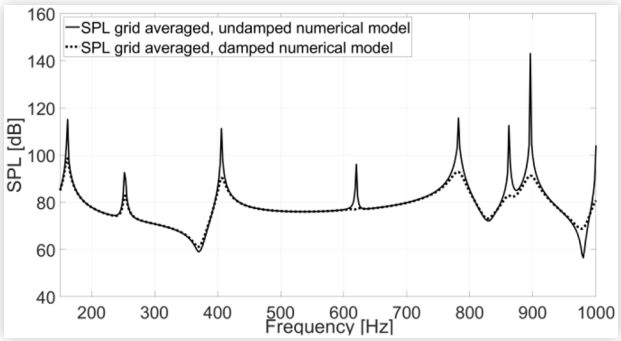

V. Force Application Point Optimization

The position of the exciting force may heavily affect the frequency response of the vibrating panels, raising the interest to investigate different force application points. For this reason, it was opted to sweep the force application point on all the nodes of the first quadrant of the mesh (considering the symmetry of the plate). Since this could provide hundreds of results, depending on the plate dimensions and mesh resolution, some optimization strategies were developed to identify optimal SPL response. In Fig. 8, it is possible to see the curves obtained by exciting all the nodes of the first quadrant. In this case, the A-weighting filter was also applied, and we refer to them as SPL(A).

The basic approach is to maximize the A-weighted mean SPL, namely *SPL_avg(A)*, calculated with (16). In Fig. 9, the comparison is shown superimposing numerical and analytical results, calculated averaging over 45 observation points. In both methods, the optimal application point of the force that

FIGURE 8 SPL(A) curves obtained by exciting all the free points of the first quadrant.

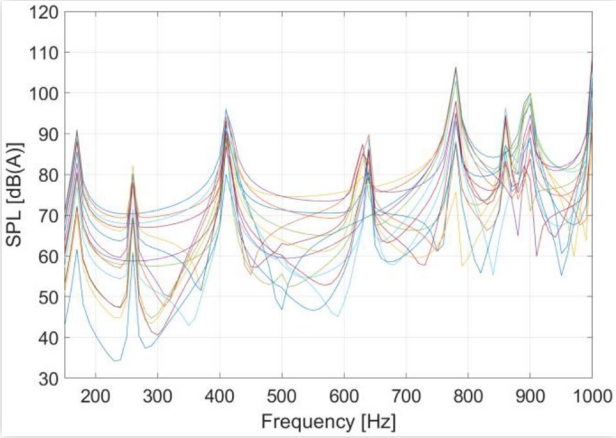

FIGURE 9 SPL(A) curves averaged over 45 observation points, maximum A-weighted Sound Pressure Level, analytical (solid line) and numerical (dash-dot line) solutions.

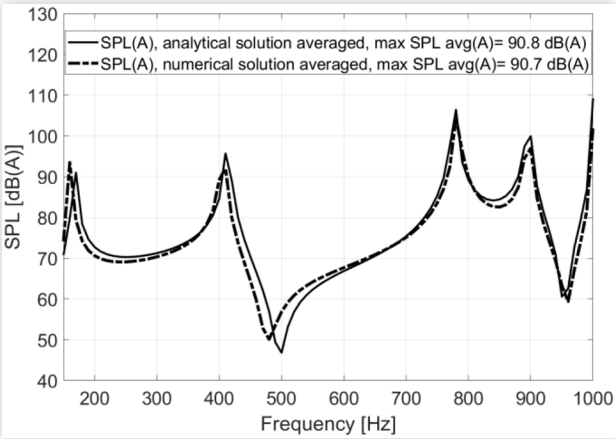

maximizes the *SPL_avg(A)* is the center of the panel. One can note that both the SPL(A) curves and the values of *SPL_avg(A)* are well matched, with $SPL\_avg(A) = 90.8\ dB(A)$ obtained from the analytical method and $SPL\_avg(A) = 90.7\ dB(A)$ obtained from the numerical method.

If one instead assumes the optimal result to have the flattest frequency response, then the best application point can be obtained by evaluating the minimum standard deviation of the A-weighted SPL curve among every excited point. The comparison of this case for the two methods is shown in Fig. 10, again averaging the results over the 45 observation points. It is possible to see also in this case a very good agreement between the two solutions: the suggested exciting point is the same, and both the curves and the *SPL_avg(A)* values are well matched, with $SPL\_avg(A) = 80.7\ dB(A)$ obtained from the analytical method and $SPL\_avg(A) = 79.1\ dB(A)$ from the numerical method. One can note that the price for having a flatter spectrum is a reduction in terms of $SPL\_avg(A)$ of about 11 dB(A), compared to the maximum sound pressure level approach.

FIGURE 10 SPL(A) curves averaged over 45 observation points, flattest spectrum, analytical (solid line) and numerical (dash-dot line) solutions.

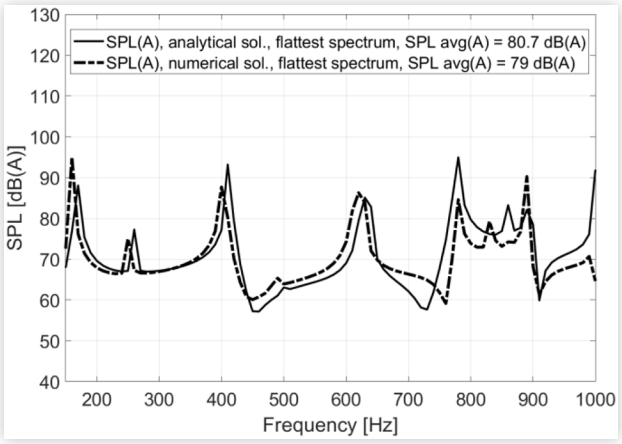

FIGURE 11 Optimal force application points, green for maximum *SPL_avg(A)* and red for flattest frequency response.

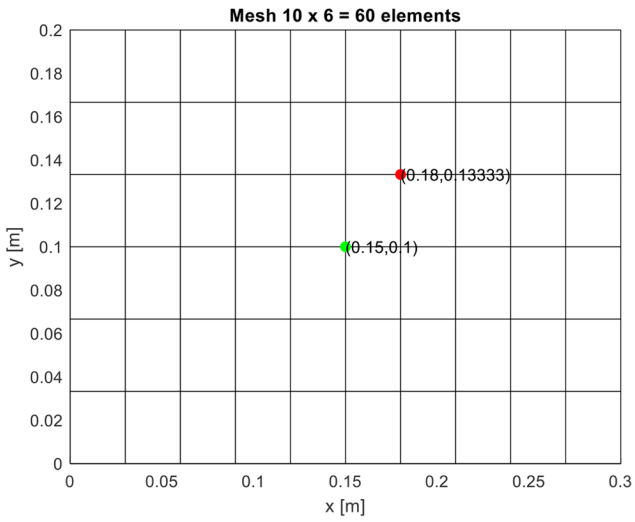

Finally, the optimization procedure allows to identify the optimal positions for the exciting force application points, which are shown in Fig. 11. As anticipated previously, the maximum *SPL_avg(A)* is obtained when the force is applied at the center of the plate (green dot). The flattest spectrum is obtained when the force is applied in correspondence of the red dot. The two optimal positions for applying the exciting force resulted identical between the analytical and numerical models, thus confirming the validity of the proposed solution.

VI. Conclusions

Fully clamped vibrating rectangular plates were investigated to assess their acoustic performance due to single harmonic excitation force.

An isotropic, un-damped aluminum plate of 0.3 m length, 0.2 m width, and 1 mm thickness was analyzed both analytically and numerically in MATLAB and COMSOL Multiphysics, respectively. The analytical method employs the Principle of Virtual Work to calculate the displacement at the nodes of a mesh, and the Rayleigh's Integral to evaluate the generated sound pressure. In both cases, the results were evaluated over a grid of points at 1 meter distance from the plate, providing more realistic and reliable results compared to the standard one point on-axis technique. The two approaches were cross validated by Sound Pressure Levels comparison, showing a very good matching between analytical and numerical methods, with differences in the range ±3 *dB*. The effect of damping was evaluated too, by introducing an isotropic loss factor in the numerical model. The result will be employed in a subsequent paper, where the authors will compare the presented methodology against experimental measurements carried out on aluminum plates with a laser-doppler vibrometer and a measurement-grade microphone.

Finally, the optimization of the position of the exciting force was studied. The central position resulted to provide the maximum total A-weighted sound pressure level, while a slightly off-center position resulted to provide the flattest frequency response. Optimal accordance between analytical and numerical solutions was pointed out in this case, too.

Acknowledgment

This research was funded by McLaren Automotive Ltd, to which the authors are grateful.

References

1. Roberts, M., Grieco, J., and Ellis, C. "Diffuse Field Radiators in Automotive Sound System Design," *AES 108th Convention*, Paris, 2000.
2. Mapp, P. and Gontcharov, V., "Evaluation of Diffuse Mode Loudspeakers in Sound Reinforcement and PA Systems," *AES 104th Convention*, Amsterdam, 1998.
3. Leissa, A.W., "The Free Vibration of Rectangular Plates," *Journal of Sound and Vibration* 31 (1973): 257-293.
4. Leissa, A.W., *Vibration of Plates* (Acoustical Society of America, 1993)
5. Leissa, A.W., "The Historical Bases of the Rayleigh and Ritz Methods," *Journal of Sound and Vibration* 287 (2005): 961-978.
6. Li, N., "Forced Vibration Analysis of the Clamped Orthotropic Rectangular Plate by the Superposition Method," *Journal of Sound and Vibration* 158, no. 2 (1992): 307-316.
7. Senjanović, I., Tomić, M., Vladimir, N., and Hadžić, N., "An Analytical Solution to Free Rectangular Plate Natural Vibrations by Beam Modes - Ordinary and Missing Plate Modes," *Transactions of famena* (2016).
8. Sung, C.C. and Jan, C.T., "Active Control of Structurally Radiated Sound from Plates," *Journal of the Acoustical Society of America* 102 (1997): 370-381.
9. Sung, C.C. and Jan, C.T., "The Response of and Sound Power Radiated by a Clamped Rectangular Plate," *Journal of Sound and Vibration Journal of Sound and Vibration* 207 (1997): 301-317.
10. Arenas, J.P., "On the Vibration Analysis of Rectangular Clamped Plates using the Virtual Work Principle," *Journal of Sound and Vibration* 206 (2003): 912-918.
11. Vlasov, V.Z., "Some New Problems on Shell and Thin Structures," *National Advisory Committee for Aeronautics* 1024 (1949).
12. Klippel, W. and Schlechter, J., "Distributed Mechanical Parameters Describing Vibration and Sound Radiation of Loudspeaker Drive Units," *125th Convention of the Audio Engineering Society*, 2008.
13. Collini, L., Farina, A., Garziera, R., Pinardi, D. et al., "Application of Laser Vibrometer for the Study of Loudspeaker Dynamics," *Materials Today: Proceedings*, 2017.
14. Oey, A., "Vibration of Rectangular Clamped Thin Plate," MATLAB Central File Exchange, [Online]. Available: https://www.mathworks.com/matlabcentral/fileexchange/28375-vibration-of-rectangular clamped-thin-plate.
15. Bellini, M.C., Collini, L., Farina, A., Pinardi, D. et al., "Measurements of Loudspeakers with a Laser Doppler Vibrometer and the Exponential Sine Sweep Excitation Technique," *Journal of the Audio Engineering Society* 65, no. 7 (2017).
16. COMSOL Multiphysics, "The Acoustics Module User's Guide," 2018. [Online]. Available: https://doc.comsol.com/5.4/doc/com.comsol.help.aco/AcousticsModuleUsersGuide.pdf.

ISSN 0148-7191